Best detection wavelength bands selection method based on multispectral radiation difference

Shu Rui[1,2], Zhou Yanping[2], Lu Chunlian[2]

(1. Shanghai Institute of Satellite Engineering, Shanghai 200240, China;
2. School of Astronautics, Harbin Institute of Technology, Harbin 150001, China)

Abstract: In low SNR cases, the distinction between spatial point-target and interferences like decoys is still a very difficult problem, especial between the satellites target and mooring decoys. At that time decoys have the same orbit and similar shape with the spatial target, so that only could be used to distinguish the target is the radiation difference. However it is not easy to extract the multi-spectral radiation which is influenced by the detection distance and observation angle. In this paper, based on the characteristics that target and interferences like decoys and noise have different radiation intensity and radiation changing frequency, the concept of the equivalent blackbody temperature in several bands (EBTSB) was built. Then the calculation model of EBTSB was designed, which could effectively reduce the interference of the space environment and fully showed the radiation differences between point-target and interferences like decoys. Under noises interference, this model would produce calculation error, and different bands combinations had different error transmission capacity. In order to make error minimum, the best detection bands need to be determined. In this paper, the best detection dual-bands and the best detection multi-bands were obtained by calculating the trend of error with the band parameters under noises interference. By analyzing the results of the simulation experiments, the best detection dual-band will have 20% advantage and the best detection multi-bands will further reduce error 20%, which prove the correctness of the conclusions of this paper.

Key words: best detection bands; equivalent blackbody temperature in several bands(EBTSB); spatial point-target; decoy

CLC number: TN215 Document code: A Article ID: 1007-2276(2014)08-2505-08

基于多光谱辐射特性差异的最佳探测波段的确定方法

舒 锐[1,2],周彦平[2],卢春莲[2]

(1.上海卫星工程研究所,上海 200240; 2. 哈尔滨工业大学 航天学院,黑龙江 哈尔滨 150001)

摘 要:低信噪比情况对空间点目标的识别仍然是很困难的问题,尤其在区分卫星目标和系留诱饵等干扰时尤为困难。此时系留诱饵与目标具有相同的运动轨迹和相似的外形特性,因而所能利用的差异仅有辐射特性差异。然而提取多光谱辐射差异并不是简单的问题,尤其是辐射会受到探测距离、探测角度

收稿日期:2013-12-02; **修订日期**:2014-01-24

作者简介:舒锐(1977-),男,高级工程师,博士,主要从事空间目标探测与识别技术、遥感卫星图像配准与目标定位技术等方面的研究。Email:shurui@126.com

的影响。基于目标和诱饵等干扰具有不同辐射强度及辐射变化频率的特点,建立了空间目标等效黑体温度的概念。并相应的设计了等效黑体温度的计算模型,该模型可以有效的减小空间环境的干扰而充分体现目标和诱饵等干扰的辐射差异。然而由于噪声的干扰,此模型会产生计算误差,并且不同的探测波段组合具有不同的误差传递能力。为了使这种噪声引起的误差最小,需要确定最佳的探测波段。通过计算噪声存在情况下,误差随探测波段参数的变化趋势,获得了最佳探测双波段、最佳探测多波段和最佳探测波段数。通过分析仿真实验的结果,使用最佳探测双波段可以减小 20%的误差,而最佳探测多波段会进一步的减小 20%的误差,这种结果证明了文中研究结论的正确性。

关键词:最佳探测波段; 多波段等效黑体温度; 空间目标; 诱饵

0 Introduction

After years of research on target detection, many methods have been developed. These include background suppression, track detection, hypothesis testing and spectral analysis. The most serious problem is to effectively distinguish between the target and decoys and noise[1-2]. In 1993, R. Haberstroh showed that light objects produced a higher brightness frequency than heavier objects due to both their light weight and their eccentric weight distribution[3]. In 1998, G. L. Silberman concluded that light objects were different from heavier objects not only in brightness frequency but also in brightness value[4]. Both papers present an idea to distinguish the target from decoys, stars, noise and so on. Both focus on the energy variation of the target in each band, and ignore the spectral relationships, which in our opinion better shows the properties of target. In this paper, the concept of equivalent blackbody temperature is presented to describe the multispectral correlation of the target, and then the principles of the best dual-bands and the combination in multi-bands are obtained through analyzing the measuring accuracy.

1 Concept of the equivalent blackbody temperature in several bands

The spatial target consists of many units which have different emissivity, reflectivity, thermal-conductivity coefficient and mass. The radiative behavior of the whole target is calculated by integrating the radiation from all units. So the radiation of the target is influenced by the rotation of the target, heat conduction, solar radiation and so on[5-7].

The whole radiation of the target is as follow.

$$\mathbf{M}_A=\sum_{n=0}^{N}\mathbf{M}_n(\varepsilon_n,\gamma_n,\delta_n,\mathbf{w}_n) \tag{1}$$

Where $\mathbf{M}_A$ is the whole radiation exitance of the target. $\mathbf{M}_n$ is the radiation exitance of unit $\mathbf{n}$. ε_n is the emissivity of the unit $\mathbf{n}$. γ_n is the reflectivity of the unit $\mathbf{n}$. δ_n is the thermal-conductivity coefficient of the unit $\mathbf{n}$, and $\mathbf{w}_n$ is the mass of the unit $\mathbf{n}$.

It is clear that the accumulation of the target radiation can not be completed accurately from all units, thus we hope to find a blackbody whose radiation approximately equals the whole radiation of the spatial target in several bands. The blackbody is defined as the equivalent blackbody of the target in several bands, and the temperature of the blackbody is EBTSB of the target.

According to Eq.(1) the EBTSB of the target is influenced by the radiant exitance of each unit, thus the EBTSB can describe the status of the target, and then show the radiation characteristic of the target. So we can utilize the radiation difference for identifying the target.

2 Measuring method of EBTSB in dual-bands

According to the Planck's law of radiation, the radiant exitance ratio of the blackbody whose EBTSB is $\mathbf{T}_0$ between Band One($\mathbf{a}_1$~$\mathbf{a}_1$+$\mathbf{b}_1$) and Band Two($\mathbf{a}_2$~

a_2+b_2) is

$$B=\frac{K_1(T_0)}{K_2(T_0)}=\frac{\int_{a_1}^{a_1+b_1}\frac{c_1}{\lambda^4\cdot\lambda[\exp(c_2/\lambda T_0)-1]}\cdot d\lambda}{\int_{a_2}^{a_2+b_2}\frac{c_1}{\lambda^4\cdot\lambda[\exp(c_2/\lambda T_0)-1]}\cdot d\lambda} \quad (2)$$

We establish the $R(T)$ curve according to the relationship between EBTSB and the ratio B. Figure 1 shows the $R(T)$ of the blackbody in 5-8μm and 10-16μm.

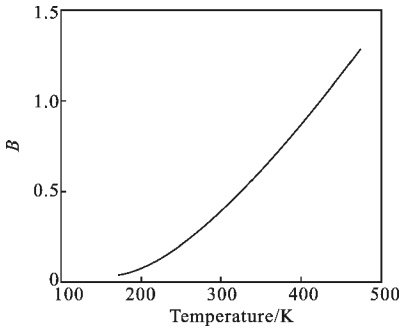

Fig.1 $R(T)$ curve

According to $R(T)$ curve, the calculation process of the EBTSB is as follow.

(1) After the detection bands are determined, we establish $R(T)$ curve according to Eq.(2);

(2) After getting the target radiation energy from detection system at time t_0 in each band, we calculate the ratio $B(t_0)$ in dual-bands;

(3) Calculating the EBTSB corresponding to $B(t_0)$ by interpolation methods.

3 Influence of noise on the measuring accuracy of EBTSB

Here we consider how noise affects the accuracy of measurement of EBTSB.

3.1 Two variables defined to describe the measuring accuracy of EBTSB

Eq.(2) is the ideal radiation ratio without noise or error. So under noises interference, we propose a new function to replace $B(T,t)$, which is as follow.

$$B_n(T,t)=\frac{G_1(t)}{G_2(t)}=\frac{K_1(T)+x_1(t)}{K_2(T)+x_2(t)} \quad (3)$$

$$G_1(t)=K_1(T)+x_1(t) \quad G_2(t)=K_2(T)+x_2(t) \quad (4)$$

Where $G_1(t)$ is the receiving energy on the detector in Band One, $K_1(T)$ is the energy of the target in Band One, and $x_1(t)$ is the energy of the noise in Band One.

After $B_n(T,t)$ is obtained, we use $R(T)$ to calculate $\hat{T}$. It is clear that the difference between $\hat{T}$ and the correct EBTSB (T_c) shows the measuring accuracy of the temperature. Two variables are defined to describe the measuring accuracy of EBTSB.

(1) Error between the mean of the temperature sequence and the correct temperature(EMTCT) is

$$\Delta T=E(\hat{T})-T_c \quad (5)$$

Where $E(\hat{T})$ is the mathematical expectation of $\hat{T}$ sequence.

(2) Distribution range of the temperature sequence around the center (RTAC) is

$$\sigma_T=\sqrt{D(\hat{T})} \quad (6)$$

Where $D(\hat{T})$ is the variance of $\hat{T}$ sequence.

EMTCT means the inherent measurement error with noise after the selection of the detecting bands. Hence if we want to detect a target whose correct EBTSB is T_c, the expected temperature should be $T_c+\Delta T$.

RTAC means the distribution range of the calculated temperatures sequence around the center after the selection of the detecting bands. That is to say, if we want to detect a target whose correct EBTSB is T_c, the temperature to be detected should be $T_c+\Delta T$, and the standard variance of temperature sequence is σ_T.

3.2 Calculation of EMTCT and RTAC

After the target and the detection bands are determined, $K_1(T)$ and $K_2(T)$ are known. Because $x_1(t)$ and $x_2(t)$ are independent random sequences with identical distribution, $G_1(t)$ and $G_2(t)$ are also independent random sequences, but their mathematical expectations are different.

Because linear interpolation is used to calculate the temperature $\hat{T}$, ΔT is estimated as $1/R'(T)\cdot\{E[B_n(T)]-B(T)\}$ and σ_T as $|1/R'(T)|\cdot\{D[B_n(T)]\}^{1/2}$.

Thus, once we get $E[B_n(T)]$, $D[B_n(T)]$ and $R'(T)$, ΔT and σ_T will be calculated.

$$E[B_n(T)]=E\left[\frac{G_1(t)}{G_2(t)}\right]=E[G_1(t)]\cdot E\left[\frac{1}{G_2(t)}\right] \quad (7)$$

$$D[B_n(T)]=E[G_1^2(t)]E\left[\frac{1}{G_2^2(t)}\right]-E^2[G_1(t)]\left[E\frac{1}{G_2(t)}\right]^2 \quad (8)$$

The noises in high-speed infrared detectors are thermal noise and shot noise, which are spectrally "white". Thermal noise is dominant[8]. So the noise components in an infrared detector are zero mean Gaussian white noise. Under these circumstances, the probability density functions of $x_1(t)$ and $x_2(t)$ are Gaussian, with a theoretical range of integration from $-\infty\sim+\infty$. It is clear that $(-\infty\sim+\infty)$ is ineffective and then the range of integration needs to be adjusted to represent a real physical situation. We take a range of integration, $IR=(-4\sigma\sim4\sigma)$, and the new probability density function becomes

$$p_x(x)=\frac{1}{0.9999\cdot\sigma\sqrt{2\pi}}\exp\left(-\frac{x^2}{2\sigma^2}\right) \quad (9)$$

Then, $E[B_n(T)]-B(T)=$

$$K_1(t)\left\{\int_{IR}\left[\frac{1}{K_2(T)+x_2(t)}\right]\cdot p_x(x)dx-\frac{1}{K_2(T)}\right\} \quad (10)$$

$$D[B_n(T)]=\int_{IR}\frac{K_1^2(T)+\sigma^2}{[K_2(T)+x_2(t)]^2}p_{x2}(x)dx-\left[\int_{IR}\frac{K_1(T)}{K_2(T)+x_2(t)}p_{x2}(x)dx\right]^2 \quad (11)$$

After the bands are selected to detect the spatial point target, $R'(T)$ is unique and its equation is

$$R'(T)=\left[\frac{K_1(T)}{K_2(T)}\right]'=\frac{K_1(T)}{K_2(T)}\left(\frac{K_1'}{K_1}-\frac{K_2'}{K_2}\right) \quad (12)$$

Finally, $\Delta T=\frac{1}{f(T)}\cdot Q(T,t)\quad \sigma_T=\left|\frac{1}{f(T)}\right|\cdot\sqrt{H(T,t)}$ (13)

Where,

$$f(T)=K_1'/K_1-K_2'/K_2 \quad (14)$$

$$Q(T,t)=\int_{IR}M(T,t)\cdot p_x(x)dx-1 \quad (15)$$

$$H(T,t)=\left(1+\frac{\sigma^2}{K_1^2}\right)\int_{IR}M^2(T,t)\cdot p_x(x)dx-[\int_{IR}M(T,t)\cdot p_x(x)dx]^2 \quad (16)$$

$$M(T,t)=\frac{K_2(T)}{K_2(T)+x_2(t)} \quad (17)$$

4 Best detection dual-bands

According to Eq.(13), ΔT and σ_T are influenced by $K_1(T)$, $K_2(T)$, K_1'/K_1, K_2'/K_2 and σ. σ is the standard variance of detector noise, so σ is constant when the type of detector and the bands are determined. The remaining five variables are T (the temperature of the target), a_1(the initial wavelength of Band One), b_1(the bandwidth of Band One), a_2 (the initial wavelength of Band Two), b_2(the bandwidth of Band Two). Finally the influencing factors are focused on T, a_1, b_1, a_2 and b_2.

4.1 Trends of EMTCT and RTAC

The relationships are calculated between ΔT, σ_T and a_1, b_1, a_2, b_2 according to Eq.(13).

(1) The relationship between ΔT, σ_T and a_1, b_1, a_2, b_2

Several trends of ΔT are illustrated in Figure 2-5 for targets with different EBTSB. ΔT increases monotonically with a_1 and b_1, and decreases monotonically with b_2. It should be noted that the relationship between ΔT and a_2 (as shown in Fig.4), and the position of minimum ΔT is determined by the temperature of target to be detected. The principle of minimum ΔT is that a_1 and b_1 are set as small as possible, and b_2 is set as large as possible. Finally a_2 should be calculated according to Eq.(13) after the target and the detecting bands are selected.

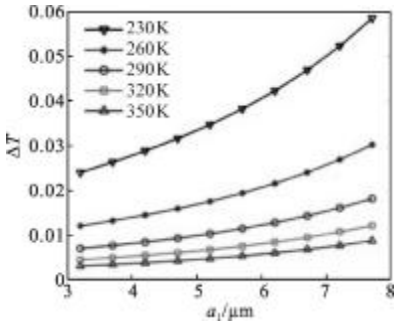

Fig.2 Relationship between ΔT and a_1

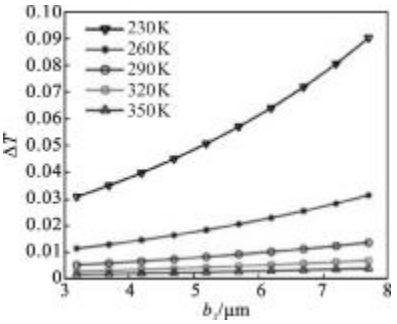

Fig.3 Relationship between ΔT and b_1

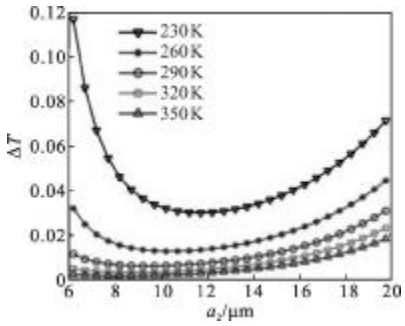

Fig.4 Relationship between ΔT and $\mathbf{a}_2$

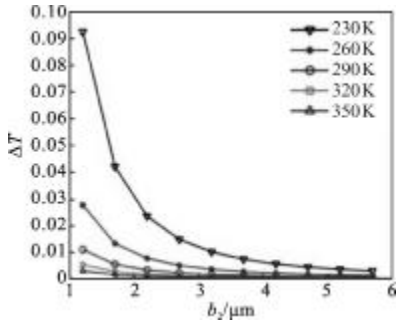

Fig.5 Relationship between ΔT and $\mathbf{b}_2$

4.2 Trend of RTAC

Figure 6-9 show the relationships between σ_T and $\mathbf{a}_1$, $\mathbf{b}_1$, $\mathbf{a}_2$, $\mathbf{b}_2$ for targets with different EBTSB. σ_T decreases monotonically with $\mathbf{a}_2$ and $\mathbf{b}_2$, and increases after the first decrease with the increase of $\mathbf{a}_1$ and $\mathbf{b}_1$.

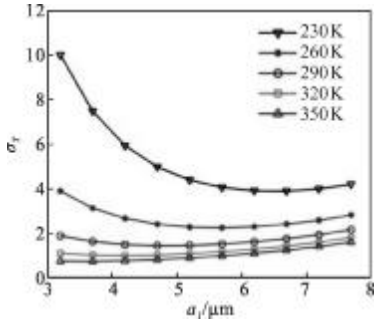

Fig.6 Relationship between σ_T and $\mathbf{a}_1$

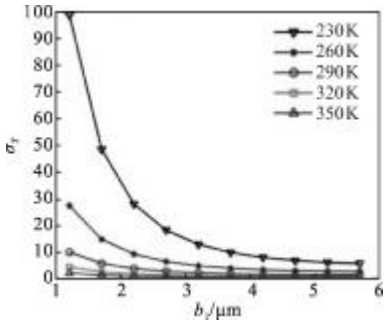

Fig.7 Relationship between σ_T and $\mathbf{b}_1$

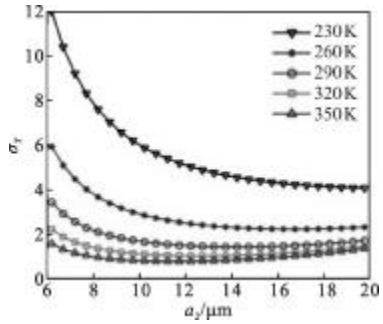

Fig.8 Relationship between σ_T and $\mathbf{a}_2$

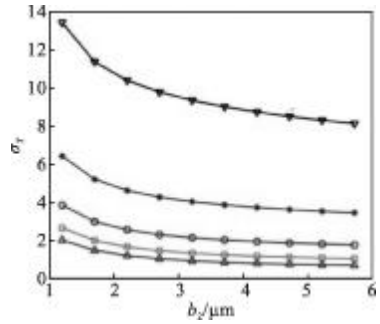

Fig.9 Relationship between σ_T and $\mathbf{b}_2$

The principle of minimum σ_T is that $\mathbf{a}_2$ and $\mathbf{b}_2$ are set as large as possible, and $\mathbf{a}_1$, $\mathbf{b}_1$ should be determined according to Eq.(13).

The best dual-bands are required in which σ_T and ΔT are minimum when detecting the spatial target. Unfortunately the trends of ΔT are different from σ_T, so the main factor should firstly be determined, then analyzed to calculate the best dual-bands. According to the definitions of ΔT and σ_T, ΔT shows the inherent error due to noise in measurement of the target, then ΔT can be considered a part of system errors after the target and the dual-bands are known. So σ_T is the only factor to be considered to determine the best dual-bands. In summary, the principle of the best dual-bands firstly minimises σ_T through the analyses of $\mathbf{a}_1$, $\mathbf{b}_1$, $\mathbf{a}_2$, $\mathbf{b}_2$, and then consideration of the minimization of ΔT follows. All things considered, the best dual-bands include $\mathbf{a}_2$ and $\mathbf{b}_2$ should be as large as possible, and $\mathbf{a}_1$ and $\mathbf{b}_1$ are determined according to Eq.(13).

As an example, the best dual-bands are $\mathbf{a}_1$=4, $\mathbf{b}_1$=4, $\mathbf{a}_2$=13, $\mathbf{b}_2$=4 when detecting a 290 K target, ΔT=0.4282, σ_T=10.018.

5 Best detection multi-bands

5.1 Measuring method of EBTSB in multi-bands

When multi-bands are used to detect the target, ΔT and σ_T should be further decreased.

There are two kinds of combinations of multi-bands.

(1) The First method is pairwise combinations of multi-bands, and each dual-band will produce an EBTSB. So if M bands are used to detect the spatial target, the quantity of EBTSB will be $M(M-1)/2$ by pairwise combinations. The final EBTSB is the mean value of the EBTSB sequence.

In this method, $M(M-1)/2$ dual-bands also produce $M(M-1)/2$ ΔT and σ_T. It is clear that ΔT and σ_T values are minimized by the best choice of bands. The calculation of the final EBTSB will add other larger ΔT and σ_T into the best dual-bands. So the measuring accuracy of the final EBTSB will increase in multi-bands, and then this method is ineffective.

(2) The second method is the combination of multi-bands into new dual-bands, and then the measuring method in dual-bands can be used to calculate EBTSB in multi-bands.

In this method, multi-bands are divided into two groups, and the energies in the bands of each group are superimposed according to proper rules. Each group will be treated as a new band, and then the additive energies in each group is the energy in the new band. So Eq.(13) are used to calculate EBTSB, ΔT and σ_T in multi-bands. In this way it is possible to significantly reduce the values of $Q(T,t)$, $H(T,t)$ and $1/f(T)$, therefore values of ΔT and σ_T will also be decreased, thus improving the measuring accuracy.

5.2 Trend analyses of $Q_M(T,t)$ and $H_M(T,t)$

Multi-bands are divided into new dual-bands, in which the energies are as follows.

$$G_{M1}(t)=\sum_{i=1}^{m}A_iK_{1i}(T)+\sum_{i=1}^{m}A_ix_{1i}(T)$$

$$G_{M2}(t)=\sum_{j=1}^{n}B_jK_{2j}(T)+\sum_{j=1}^{n}B_jx_{2j}(T) \tag{18}$$

Where, $K_{1i}(T)$ is an integral part of the energies of target in new Band One, and $x_{1i}(T)$ is an integral part of the energies of noises in new Band One. A_i is the combination coefficient of new Band One, and B_j is the combination coefficient of new Band Two.

After equations derivation,

$$\Delta T_M=\frac{1}{f_M(T)}\cdot Q_M(T,t)\quad \sigma_{TM}=\left|\frac{1}{f_M(T)}\right|\cdot\sqrt{H_M(T,t)} \tag{19}$$

$$\text{Where, } f_M(T)=\frac{\sum_{i}^{M}A_iK_{1i}'(T)}{\sum_{i}^{M}A_iK_{1i}(T)}-\frac{\sum_{j}^{N}B_jK_{2j}'(T)}{\sum_{j}^{N}B_jK_{2j}(T)} \tag{20}$$

$$Q_M(T,t)=\iint_n M_M(T,t)\cdot p_{x1}dx_1\cdots p_{xn}dx_n-1 \tag{21}$$

$$H_M(T,t)=[1+N_M(T,t)]\cdot\iint_n M_M^2(T,t)\cdot p_{x1}dx_1\cdots p_{xn}dx_n-\left[\iint_n M_M(T,t)\cdot p_{x1}dx_1\cdots p_{xn}dx_n\right]^2 \tag{22}$$

$$M_M(T,t)=\frac{\sum_{j=1}^{n}B_jK_{2j}(T)}{\sum_{j=1}^{n}B_jK_{2j}(T)+\sum_{j=1}^{n}B_jx_{2j}(T)} \tag{23}$$

$$N_M(T,t)=\frac{\sum_{i=1}^{m}A_i^2\sigma_{1i}^2}{\left[\sum_{i=1}^{m}A_iK_{1i}(T)\right]^2} \tag{24}$$

According to Eq.(19),

(1) When $\sum_{j}^{N}B_jK_{2j}(T)/\sum_{j}^{N}B_j$ increasing, both $Q_M(T,t)$ and $H_M(T,t)$ will decrease.

(2) When $\sum_{i=1}^{m}A_iK_{1i}(T)/\sqrt{\sum_{i}^{m}A_i^2}$ increasing, $H_M(T,t)$ will decrease and $Q_M(T,t)$ doesn't change.

That is to say when

$$\sum_{i=1}^{m}A_iK_{1i}(T)>\sqrt{\sum_{i}^{m}A_i^2}\cdot\frac{K_{11}(T)}{\sigma_{11}},$$

$$\sum_{j=1}^{n}B_jK_{2j}(T)>\sum_{j=1}^{n}B_j\cdot K_{21}(T) \tag{25}$$

$Q_M(T,t)<Q(T,t)$ and $H_M(T,t)<H(T,t)$.

Where, $K_{11}(T)$ is the energy in Band One of dual-bands and $K_{21}(T)$ is the energy in Band Two of dual-bands.

5.3 Trend analysis of 1/f(T)

The f(**T**) in dual-bands is

$$f_\theta(\mathbf{T})=\frac{\mathbf{K}_{11}'}{\mathbf{K}_{11}}-\frac{\mathbf{K}_{21}'}{\mathbf{K}_{21}} \tag{26}$$

The f(**T**) in multi-bands is

$$f_M(\mathbf{T})=\frac{\sum_{i=1}^{m}\mathbf{A}_i\mathbf{K}_{1i}'(\mathbf{T})}{\sum_{i=1}^{m}\mathbf{A}_i\mathbf{K}_{1i}(\mathbf{T})}-\frac{\sum_{j=1}^{n}\mathbf{B}_j\mathbf{K}_{2j}'(\mathbf{T})}{\sum_{j=1}^{n}\mathbf{B}_j\mathbf{K}_{2j}(\mathbf{T})} \tag{27}$$

When Eq.(26) is satisfied $1/f_M(\mathbf{T})<1/f_\theta(\mathbf{T})$, then

$$\frac{\sum_{i=2}^{m}\mathbf{A}_i\mathbf{K}_{1i}'(\mathbf{T})}{\sum_{i=2}^{m}\mathbf{A}_i\mathbf{K}_{1i}(\mathbf{T})}>\frac{\mathbf{K}_{11}'}{\mathbf{K}_{11}},\quad \frac{\sum_{j=2}^{n}\mathbf{B}_j\mathbf{K}_{2j}'(\mathbf{T})}{\sum_{j=2}^{n}\mathbf{B}_j\mathbf{K}_{2j}(\mathbf{T})}<\frac{\mathbf{K}_{21}'}{\mathbf{K}_{21}} \tag{28}$$

Finally when Eq.(25) and (28) are satisfied, the measuring accuracy in multi-bands is better than in dual-bands.

To verify the analysis of this paper, our method is applied to the detection of a 290 K target. The results are given in Tab.1.

Tab.1 Measuring accuracy in several combinations of multi-bands

	Method in dual-bands				First method in multi-bands	Second method in multi-bands
Detection bands combination /μm	3-7 13-17	3-7 14-19	4-8 13-17	4-8 14-19	3-7, 4-8 13-17, 14-19	3-7, 4-8 13-17, 14-19
$\Delta\mathbf{T}$	0.3533	0.2932	0.4282	0.3518	0.3566	0.1784
σ_T	12.663	11.935	10.018	9.238	10.964	7.484

In Tab.1, the measuring accuracy of the second method is the best, which has a 20% advantage than the best dual-bands. The result of the first method is poor and matches the analysis of paper well. The measuring accuracies in four dual-bands also prove the principle of the best dual-bands. All things considered, the results in Tab.1 are in accordance with the analyses of this paper.

6 Best quantity of the detection bands

From the result in Tab.1, we know the best detection multi-bands will reduce the error than the best dual-bands, but how many bands will make the error minimum and whether the more bands used, the more minimum the error is.

Figure 10 shows the relationship between the number of detection bands and $\Delta\mathbf{T}$ and σ_T, from which we know that in the initial period the number of detection bands increased $\Delta\mathbf{T}$ and σ_T decrease, but with the number of detection bands increases to certain extent $\Delta\mathbf{T}$ and σ_T will not further decrease. That is to say the increase of the number of detection bands would not improve the measuring accuracy of EBTSB, we need reasonably choose the number of detection bands according to the characteristics of the target detected.

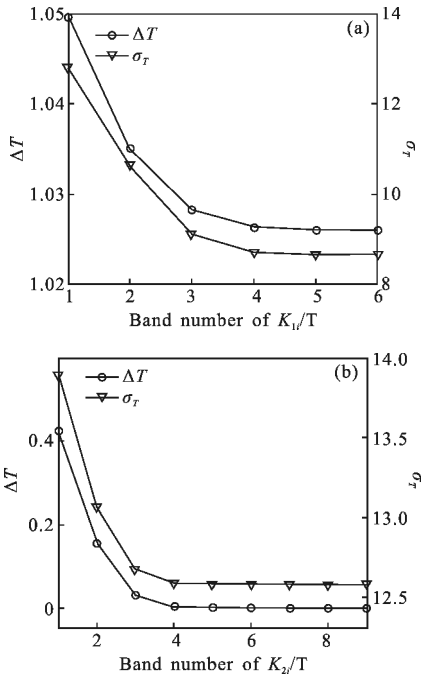

Fig.10 Influence of the band number on $\Delta\mathbf{T}$ and σ_T

7 Conclusions

In this paper we defined the concept of EBTSB and calculation model of EBTSB, which can effectively reduce the interference of the space

environment and fully show the radiation differences between point-target and inter ferences like decoys. And then multispectral correlation of the target was analyzed to get the best bands. The following conclusions are reached:

(1) Different **R**(**T**) curves have different error transfer ability, which can be minimum by selecting the detection bands.

(2) The best dual-bands include $\mathbf{a}_2$ and $\mathbf{b}_2$ should be as large as possible, and $\mathbf{a}_1$ and $\mathbf{b}_1$ are determined according to Eq.(13).

(3) When Eqs. (25), (28) are satisfied, the measuring accuracy in multi-bands will be better than in best dual-bands.

(4) Increase of the number of detection bands would not improve the measuring accuracy of EBTSB, we need reasonably choose the number of detection bands according to the characteristics of the target detected.

References:

[1] Yang Fan, Xuan Yimin, Han Yuge. Analysis of SNR for ground-based infrared detection of space object [J]. Infrared and Laser Engineering, 2012, 41(11): 2879-2885. (in Chinese)

[2] Sun Chengming, Yuan Yan, Huang Fengzhen, et al. Modeling and simulation on infrared imaging characteristics of space target [J]. Infrared and Laser Engineering, 2012, 41(3): 563-568. (in Chinese)

[3] Haberstroh R, Kadar I. Multi-spectral data fusion using neural networks[C]//SPIE, 1993, 1955: 65-75.

[4] Silberman G L. Parametric classification techniques for theater ballistic missile defense [J]. Johns Hopkins Apl Technical Digest, 1998, 19: 322-339.

[5] Wang Ying, Lai Xiaoyi, Huang Jianming, et al. Infrared radiation analysis of space target based on Sinda/G and Matlab [J]. Infrared and Laser Engineering, 2012, 41(5): 1113-1118. (in Chinese)

[6] Xu Hui, Sun Zhongkang. Temperature fields of the surfaces of satellite and its decoy [J]. Journal of National University of Defense Technology, 1994, 16(3): 12-18. (in Chinese)

[7] An Wei, Xu Hui, Li Hong, et al. IR point target based feature extraction and recognition on thermophysics analysis [J]. Journal of National University of Defense Technology, 1998, 20(6): 46-50. (in Chinese)

[8] Shu Rui, Zhou Yanping, Tao Kunyu, et al. The simulation of the receiving of the spatial infrared detector [J]. Journal of Harbin Institute of Technology, 200, 39 (S1): 237-240. (in Chinese)